Research Paper
Journal of Aerospace System Engineering
Vol.15, No.2, pp.10-15 (2021)
EISSN 2508-7150
http://dx.doi.org/10.20910/JASE.2021.15.2.15

Downward Load Prediction and Reduction Strategy for QTP UAV

Youngmin Park†, Jaehoon Choi, Hakmin Lee and Cheolwan Kim
† *Aeronautics Technology Research Division,*
Korea Aerospace Research Institute

Abstract

The propeller wake of tiltrotor-type aircrafts, such as TR-60 and quad tilt propeller (QTP) UAV, in hover substantially impinges the upper surface of the primary wing and generates a downward load. This load is directly proportional to the thrust of the propeller and reduces the available payload. Therefore, wing and nacelle mechanisms should be carefully designed to reduce downward load. This study conducted a numerical analysis of the rotating propeller in hover to predict the downward load of a QTP UAV. An unsteady three-dimensional Navier−Stokes solver was used along with a sliding mesh for the simulation of the rotating propeller. To reduce the downward load, the tilting mechanisms of the partial wing and nacelle were simultaneously introduced and numerically analyzed. Finally, the downward load was predicted by 14% of isolated propeller thrust; further, the downward load could be reduced by adopting the partial wing and nacelle tilting concept.

Key Words : Tiltrotor, Quad Tilt Propeller, UAV, Hovering, Downward Load, Unsteady, Computational Fluid Dynamics

1. Introduction

Tiltrotor-type aircrafts, such as TR-60 and quad tilt propeller (QTP), exhibit the same advantages as those exhibited by fixed-wing and rotary-wing aircrafts, as the propeller mounted at the end of the wing of tiltrotor-type aircrafts can be tilted according to flight conditions. However, the strong wake of the propeller generated under high-thrust conditions while hovering may collide with the wing, resulting in a downward load in the opposite direction to the propeller thrust. Since the downward load of the tiltrotor-type aircraft is the largest factor that reduces the aircraft thrust in hover, various analytical and experimental studies have been conducted to accurately predict and decrease the downward load during conceptual and initial design processes. A key experimental and analytical study on the downward load was undertaken in the late 1980s [1]. In this literature, the wing and propeller configurations of V-22 were tested at the Outdoor Aerodynamic Research Facility of NASA, and the thrust and downward load properties were estimated. A low downward load ratio of 8-10% was measured for the V-22 configuration at the flap deflection of 60°, and the downward load was increased to 16% when the flap deflection was set at 0°. The aerodynamic interference test of the scaled proprotor and wing configurations of V-22 can be found in Reference [2]. In the literature, various geometrical combinations of wing incidence angle, flap angle, distance between prop wings, and rotational direction were tested and compared, and the downward load was predicted to be approximately 10% at the flap deflection of 75°. A downward load test was also conducted in a wind tunnel (40 ft x 80 ft) at the NASA Ames Research Center, wherein the downward load was calculated to be 8% at the flap angle of 75° [3].

Computational analysis has been actively utilized for making predictions since the 1980s with the development of computational analysis software and analysis equipment. The computational analysis of V-22 was attempted as seen in References [4, 5], which demonstrated sufficient potential for the application of computational analysis in the development of tiltrotor aircrafts. The hovering conditions of the half-span and full-span configurations of V-22 were analyzed, and the downward load was predicted via computational fluid dynamics analysis using OVERFLOW [6] based on an overset mesh technique. In the analysis, the downward load was predicted to be 13% at the flap deflection of 67° for the half-span configuration. In the field of computational analysis in South Korea, the proprotor and wing models of V-22 have been analyzed using an unstructured sliding mesh technique [7], which predicted a low downward load of approximately 8% through inviscid analysis. In South Korea, the downward load was predicted as seen in Reference [8] for the initial configuration of a smart UAV, TR-S1, using a Navier-Stokes solver. In this study, the downward load of TR-S1 was predicted to be approximately 10%. Subsequent examples of similar

Received: Aug. 06, 2020 Revised: Oct. 28, 2020 Accepted: Nov. 02, 2020
† Corresponding Author
Tel: +82-42-860-2692, E-mail: ympark@kari.re.kr

computation analysis include a study on the performance improvement of tiltrotor aircraft using extended wings [9] and studies on mounting atmospheric data sensors and improving the aerodynamic performance of a multicopter [10, 11].

Subsequently, the focus of the computational analysis field shifted from downward load prediction to numerical techniques and turbulence models for fluid dynamics analysis [12, 13]. Recently, flow control techniques to reduce downward load were investigated, which showed that the downward load could be reduced by 30% through Active Flow Control (AFC) based on an oscillating jet [14, 15]. However, despite the AFC-based reduction of the downward load, it is difficult to apply AFC in an actual aircraft due to structural, weight, and technical limitations.

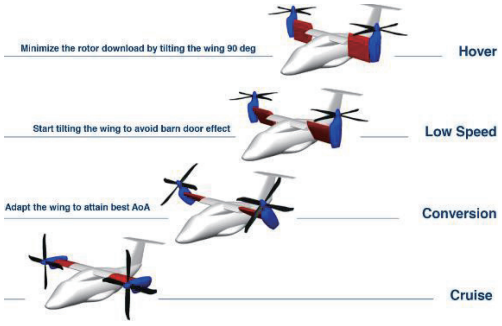

Fig. 1 ERICA Tiltrotor Operation Concept [16].

Recently, the method of rotating partial wings along with nacelles has been investigated to reduce tiltrotor downward load. The rotary-wing aircraft group in Europe has undertaken the Enhanced Rotor Craft Innovative Concept Achievement (ERICA) project to counter the tiltrotor technology led by the United States, establishing its own next-generation tiltrotor model and conducting related research [16]. The ERICA tiltrotor model comprises a small-diameter, four-blade proprotor to enable take-off and landing in the fixed-wing mode and uses the method of independently rotating partial wings with nacelles depending on the flight condition. The wind tunnel experiment, proprotor design, and computational analysis of the downward load of ERICA tiltrotors are described in detail in References [17, 18].

Fig. 2 NASA pusher proprotor tiltrotor [18].

NASA recently presented the concept of push proprotor tiltrotor (PPT) to minimize the downward load and maximize the aerodynamic performance of the Large Civil Tiltrotor (LCTR) conceptual configuration and performed a computational analysis to derive the optimal configuration (Fig. 2). The result from optimizing the PPT configuration with computational analysis indicated a reduction in the downward load to 2% [19].

Fig. 3 KARI QTP UAV

In this study, a numerical analysis was conducted on the QTP UAV (Fig. 3), which is developed and successfully flown by the Korea Aerospace Research Institute; further, the downward load properties were analyzed. The three-dimensional unsteady Navier-Stokes solver was applied for the computational analysis, and the sliding mesh method was used to simulate the propeller rotation. Further, the mesh was generated, reflecting the rotation of the partial wings and nacelles to reduce the downward load, and the effect of the degree of wing separation on the reduction of downward load was analyzed.

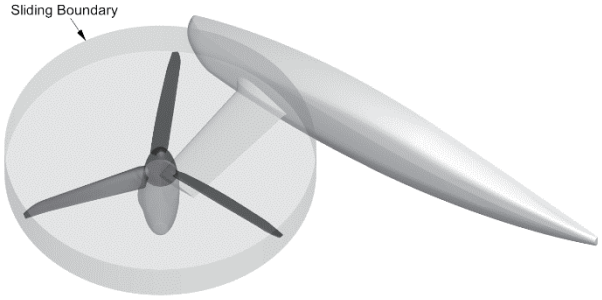

Fig. 4 QTP surface model and sliding boundary.

2. Numerical Method

2.1 Mesh Generation

The size of the QTP aircraft used in the analysis is 2,034 mm in fuselage length, 1,500 mm in front wingspan, 2,200 mm in rear wingspan, and 550 mm in propeller radius, both in the front and back. To reduce the run time of the numerical analysis, the mesh was only generated for the combination of the fuselage, front wing, nacelle, and propeller on half the QTP configuration.

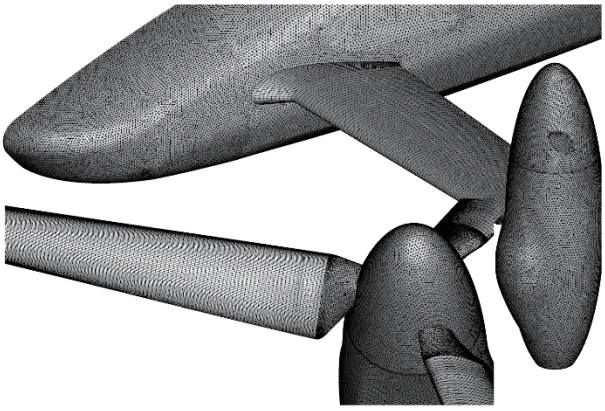

Fig. 5 Surface mesh on the wing and propeller.

The propeller was set to rotate at 1,800 rpm under hovering conditions, and the rotation boundary of the sliding mesh for simulating the propeller was constructed in the form of a cylinder with a radius 5% larger than the propeller radius. Figure 4 shows the QTP configuration and propeller, as well as the encompassing sliding boundary.

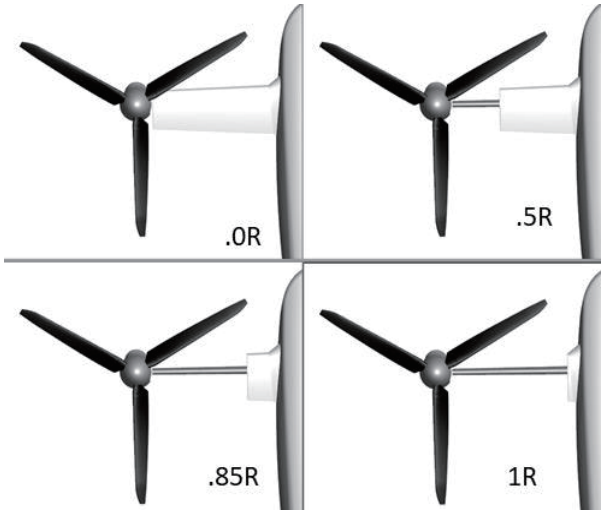

Fig. 6 Wing separations for downward load reduction.

Figure 5 shows the schematic of the generated surface mesh, including the rectangular mesh for the wing and propeller blades that provides lift and the unstructured triangular mesh for the fuselage and nacelle. Approximately 230,000 surface mesh grids exist, of which the propeller blade accounts for 45%. The generated volume grid consists of 28 million grid cells and 11 million vertices.

To examine the effect of wing separation on the downward load, the mesh was generated by separating the wing in the simulation. The wing separation was set at 50%, 85%, and 100% of the propeller radius relative to the propeller hub axis, which is depicted in Fig. 6. The effects of wing separation, shown in Fig. 6, and nacelle tilting on whirl flutter, etc. are being studied by the ADYN work group of the ERICA project through numerical analysis and testing [16].

2.2 Analysis Method

The unsteady three-dimensional Navier-Stokes solver was applied in the fluid dynamics analysis, and the spatial discretization method based on the least square method and k-ω SST turbulence model were used. In the unsteady analysis process, the time interval for each step was set at 1.667×10^{-4} s, and the propeller would complete one revolution after 200 iterative calculations. In the unsteady analysis process, the dual time-stepping method of second-order accuracy was used, and the number of sub-iterations was set at 20. The unsteady analysis method used in the analysis is described in detail in Reference [22].

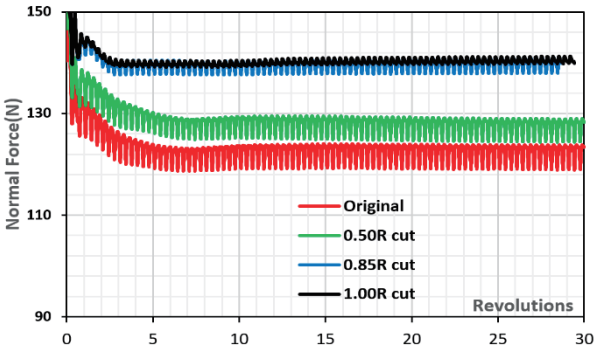

Fig. 7 Time history of normal force coefficient.

3. Analysis Results

3.1 Convergence Properties

Figures 7 and 8 show the normal and axial force coefficients of the full-scale aircraft changing with the number of revolutions in the computational analysis. In the plots, the two aerodynamic coefficients are found to converge after approximately 10 revolutions of the propeller. The normal force coefficient indicates that the downward load is almost eliminated while the propeller thrust is restored when the wing is separated at 0.85R or more.

Figure 8 is a plot of the axial force coefficient, which shows that the backload is almost non-existent with the original and 0.5R separation configurations; however, a backload of 10N occurs with 0.85R and 1.0R separation configurations. This is a phenomenon caused by the rotation of the propeller wake, resulting in an effective angle of attack on the wing and the lift component acting backward. For QTP, the front and rear propellers rotate in the opposite direction and most of the lift by the two wings is offset, which may not have a significant effect on the behavior of the aircraft under hovering conditions. However, for tiltrotors with two propellers, the use of separated

wings can cause a backload and requires countermeasures. In fact, for the ERICA tiltrotor that uses separated wings, a wing angle is suggested to prevent wing lift under hovering conditions. The backload caused by the lift of separated wings is approximately 8% of the propeller thrust and that of the ERICA tiltrotor configuration is approximately 5%.

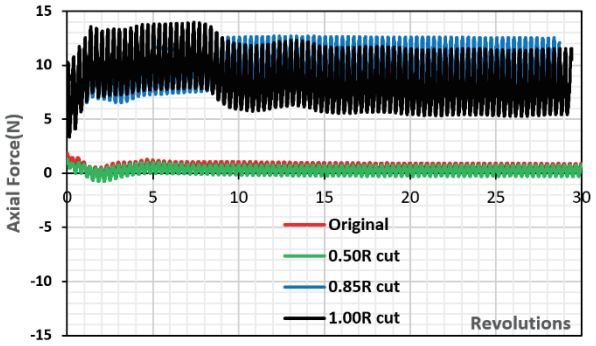

Fig. 8 Time history of axial force coefficient.

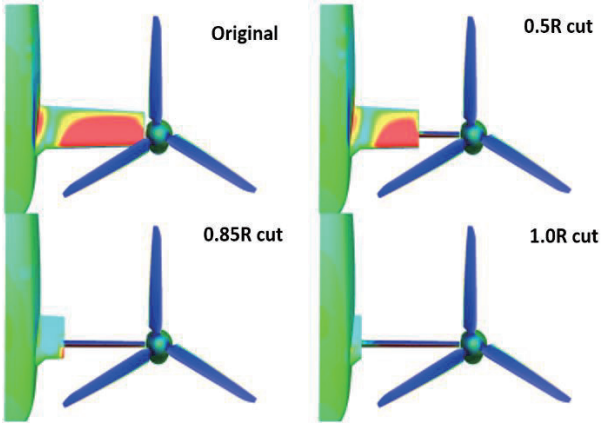

Fig. 9 Surface pressure distribution (top-view).

3.2 Surface Pressure Distribution

Figures 9 and 10 show the instantaneous pressure distribution as a function of wing separation while the propeller rotates. In these figures, a strong pressure distribution is observed on the upper surface of the wing near the fuselage, and severe interference with the fuselage also appears with the original and 0.5R separation configurations. On the contrary, the strong pressure resulting from the impingement of the wake at the fuselage and wing joint does not occur with the 0.85 and 1.0R separation configurations. Ultimately, the use of separated wings has the advantage of reducing interference with the fuselage because the propeller wake flows naturally to the bottom without impingement on the wings.

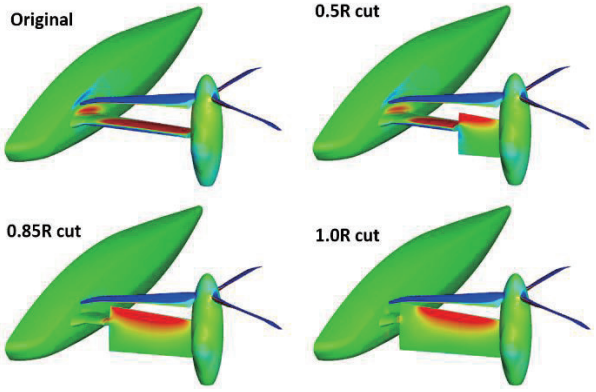

Fig. 10 Surface pressure distribution (iso-view).

3.3 Downward Load and Backload

Table 1 summarizes the downward load and backload of each wing separation configuration. First, the downward load of the 0.5R separation configuration is approximately 8.7%, with no significant improvement.

Table 1 Aerodynamic loads for each configuration.

Config	PT(N)	DL(N)	BL(N)	TT(N)	DL(%)	BL(%)
Original	142.9	19.6	1.3	123.3	13.7	0.9
0.5R	140.7	12.2	2.6	128.5	8.7	1.8
0.85R	140.8	0.6	11.8	140.2	0.4	8.4
1.0R	141.5	1.2	10.5	140.3	0.8	7.5

* PT: Propeller Thrust, TT: Total Thrust DL: Downward Load BL: Backload

However, most of the downward load was reduced, and the backload was also consistent at approximately 8% with the 0.85R and 1.0R separation configurations. Therefore, the wings should be separated at a minimum of 0.85R to realize the effect of wing separation and designed such that the 8% backload is offset by adjusting the tilt angle of the propeller or tilting the wings forward.

3.4 Comparison to ERICA Configuration

Figure 11 compares the effect of wing separation on reducing the downward load of QTP and the ERICA tiltrotor configuration [17]. The figure shows that, while the actuator disk method was used in the analysis of the ERICA tiltrotor, wherein the plane of propeller rotation was assumed to be a disk, the results obtained were similar to those obtained by the analysis conducted in this study, wherein the propeller was directly rotated. A more efficient computational analysis of downward load will be possible in the future if the actuator disk method is applied to the QTP configuration and verified by comparing it to the sliding mesh method. The variation of the downward load with wing separation indicates that the downward load is drastically reduced when the wing separation is 0.7R or more for both cases. The higher downward load of

the ERICA configuration than that of QTP under the same configuration condition with no wing separation (r/R~0.3) is attributed to the smaller propeller diameter of the ERICA configuration relative to the wings and the greater disk loading with four blades. For the same reason, the downward load appears to be slightly greater in climb than in hover. However, the effect of decreasing the downward load with wing separation tends to be very similar for both QTP and ERICA tiltrotors, which can be considered for designing similar aircraft in the future.

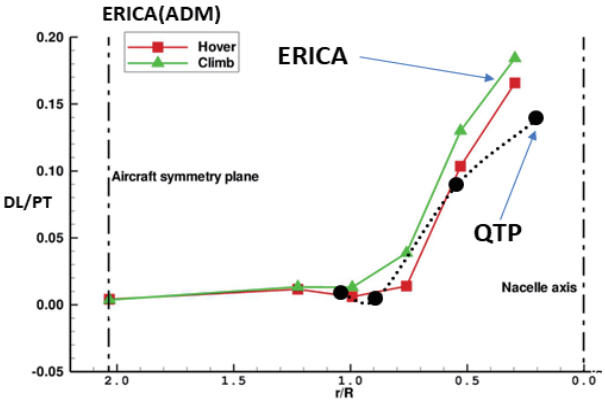

Fig. 11 Comparison of downward loads distribution for QTP and ERICA tiltrotors.

4. Conclusions

This study conducted a computational analysis on the QTP UAV propeller, and the downward load properties were analyzed. The following conclusions were drawn:

1. The downward load of the original configuration was approximately 14% of the isolated propeller thrust, which was almost eliminated by separating the wing at 0.85R and 1.0R.

2. A backload of approximately 8% of the propeller thrust occurred with 0.85R and 1.0R wing separations due to the propeller wake and the resulting wing lift.

3. The analysis of various configurations indicates that most of the downward load can be eliminated by separating the wings at 0.7R or more.

4. The comparison to prior studies shows that the results obtained for the analysis method used in this study and the actuator disk method used for the analysis of the ERICA tiltrotor were similar. The actuator disk method can be an alternative for more efficient analysis in the future.

5. As reported in other studies, since a significant downward load occurs with a large disk loading, the application of wing separation can improve the hover and climb performances of aircrafts.

Epilogue

This study is part of the major project funded by the National Research Council of Science and Technology ((Sub 4) Technological Research on Aerodynamic Performance Improvement of Multi-electric Propulsion Aircraft, Project No. FR21A04). We appreciate their support.

References

[1] M. A. McVeigh, “The V-22 tilt-rotor large scale rotor performance/wing download test and comparison with theory,” *11th* European Rotorcraft Forum, No. 97, 1986.

[2] F. F. Felker, and J. S. Light, “Rotor/wing aerodynamic interactions in hover,” NASA TM 88255, 1986.

[3] F. F. Felker, P. R. Shinoda, R. M. Heffernan, and H. F. Sheehy, “Wing force and surface pressure data from a hover test of a 0.658-scale V-22 rotor and wing,” NASA TM 102244, 1990.

[4] R. L. Meakin, “Unsteady simulation of the viscous flow about a V-22 rotor and wing in hover,” *AIAA Atmospheric Flight Mechanics Conf.*, AIAA Paper 95-3463, 1995.

[5] D. R, Poling, H. Rosenstein, and G. Rajagopalan, “Use of a Navier-Stokes code in understanding tiltrotor flowfields in hover,” *Journal of the American Helicopter Society*, vol. 43, no. 2, pp 103-109, 1998.

[6] M. A. Potsdam, and R. C. Strawn, “CFD simulation of tiltrotor configurations in hover,” *58th* American H*elicopter Society Annual Forum*, 2002.

[7] Y. Park, C. Kim, J. Lee, and O. Kwon, “Download prediction of tiltrotor by using computational fluid dynamics,” *Proc. of the 2004 KSCFD Spring Conf.*, 2004.

[8] S. Ko, S. Ahn, and B. Kim, “Numerical analysis of aerodynamic performance for tilt rotor aircraft in hovering mode,” *Journal of the Korean Society for Aeronautical and Space Sciences*, vol. 34, no. 1, pp. 8-17, 2006.

[9] M. Lee, and C. Lee, “Increasing endurance performance of tiltrotor UAV using extended wing,” *Journal of Aerospace System Engineering*, vol. 10, no. 1, pp. 111-117, 2016.

[10] Y. Park, C. Lee, and Y. Lee, “Numerical analysis of flowfield around multicopter for the analysis of air data sensor installation,” *Journal of Aerospace System Engineering*, vol. 11, no. 5, pp. 20-27, 2017.

[11] S. Hwang, Y. Park, and Y. Lee, “Cross-rotating multicopter,” *Journal of Aerospace System Engineering*, vol. 13, no. 1, pp. 47-53, 2019.

[12] J. Abras, and R. Narducci, “Analysis of CFD modeling techniques over the MV-22 Tiltrotor,” *66th American Helicopter Society Annual Forum*, 2010.

[13] N. M. Chaderjian, “Advances in rotor performance and turbulent wake simulation using DES and adaptive mesh refinement,” *7th Int. Conf. on Computational Fluid Dynamics*, ICCFD7-3506, 2012.

[14] Y. Yadlin, A. Shmilovich, and R. Narducci, “Application of

active flow control for download alleviation in rotorcraft," *35th AIAA Applied Aerodynamics Conf.*, AIAA 2017-3045, 2017.

[15] H. M. Nagib, J. W. Kiedaisch, I. J. Wygnanski, A. D. Stalker, T. Wood, and M. A. McVeigh, "First-in-flight full-scale application of active flow control: The XV-15 tiltrotor download reduction," RTO-MP-AVT-111.

[16] R. Bianco-Mengotti, "Technical challenges for the future of rotary wing: the Agusta-Westland path to the new generation tilt-rotor," http://www.aofs.org, 2012.

[17] G. Droandi, "Wing-rotor aerodynamic interaction in tiltrotor aircraft," Ph.D. Thesis of Politecnico di Milano, 2014.

[18] A. J. Garcia, and G. N. Barakos, "CFD Simulations on the ERICA tiltrotor using HMB2," *AIAA SciTech Forum*, AIAA 2016-0329, 2016.

[19] L. A. Young, "What is a tiltrotor? A fundamental reexamination of the tiltrotor aircraft design space," *Transformer Vertical Flight*, 2018.

[20] S. Hwang, and C. Kim, "Aerodynamic design of the quad-tilted VTOL UAV," *The Society for Aerospace System Engineering Fall Conf.*, 2017.

[21] Y. Park, J. Choi, and C. Kim "Numerical simulation of downloads for QTP UAV propeller," *The Korean Society for Aeronautical and Space Sciences Fall Conf.*, 2019.

[22] Y. Park, J. Choi, and Y. Lee "Numerical analysis of the flow field around multicopter," *The Korean Society for Aeronautical and Space Sciences Spring Conf.*, 2017.